

Kinematics of the Slumgullion landslide revealed by ground-based InSAR surveys

W.H. Schulz, J.A. Coe, B.L. Shurtleff & J. Panosky

United States Geological Survey, Denver, Colorado, USA

P. Farina, P.P. Ricci & G. Barsacchi

Ingegneria Dei Sistemi, Pisa, Italy

ABSTRACT: Knowledge of landslide kinematics is a basic requirement for understanding landsliding mechanisms. Traditional approaches for characterizing landslide kinematics often require centimeters-meters of landslide movement to be effective, are labor intensive, costly, time consuming, and can be dangerous or impossible on inaccessible landslides. We tested the IBIS-L, which is a ground-based, interferometric, synthetic aperture radar, to determine whether it could rapidly acquire kinematic data for the complex, 3.9-km-long Slumgullion landslide located in Colorado, USA. The landslide moves persistently at rates of \sim cm/d. Displacement data acquired by the IBIS-L, apart from some points located in vegetated areas, compared favorably with measurements made using GPS surveys and in-situ instrumentation. Within one day of surveying, kinematic elements comprising the landslide were clearly evident and correlated well with results from previous field mapping and analyses of aerial photographs. Preliminary analyses of results provide insight into characteristics of the landslide.

1 INTRODUCTION

Landslides cause thousands of casualties and billions of dollars in property damage annually (Spiker & Gori 2003). To reduce hazards from landslides, mechanisms controlling their movement must be understood. Knowledge of landslide kinematics is the most basic requirement for this understanding, and also assists characterization of landslide boundary geometry, positions of landslide elements driving and resisting motion, and variations in material properties, landslide thickness, and pore-water pressures. The movement of even simple, single blocks of sliding rock often is temporally complex, and most landslides also have spatially complex movement. Short-term and long-term temporal features of a landslide's kinematics generally are documented from in-situ monitoring using extensometers, crack meters, inclinometers, laser or sonar range finders, GPS receivers, etc. at specific locations on a landslide. Such monitoring efforts are spatially discontinuous, costly, and labor intensive. Surface manifestations of temporal and spatial variations in a landslide's kinematics can be mapped to provide a more spatially continuous kinematic characterization, but such mapping also is costly and labor intensive to perform and requires sufficient movement (generally decimeters

to meters) to be effective. Additionally, these traditional approaches for documenting landslide kinematics require access to the landslide, careful selection of proper monitoring equipment and locations for point monitoring, and weeks-months for initial site evaluations, planning, permit acquisitions, equipment installation, mapping activities, and, most importantly, sufficient landslide movement to permit the mapping and monitoring methods to be effective.

Interferometric ground-based InSAR (GB-InSAR) surveying can overcome many of the limitations inherent in traditional kinematic studies by providing autonomous, rapid acquisitions (minutes) of kinematic data at long distances (up to 4 km) and across large areas (several km²) from remote locations with displacement accuracy on the order of mm or better (e.g., Tarchi et al. 2003a, b). These surveys can be performed in any weather and lighting conditions and do not require access to the landslide for any reason, including for installation of manmade reflectors. Furthermore, kinematic data can be reduced in near real time, permitting GB-InSAR to be used for monitoring of critical slope failures and issuing of alarms when selected movement characteristics are observed. GB-InSAR is now commonly used by prominent mining groups internationally and by civil protection authorities in developed

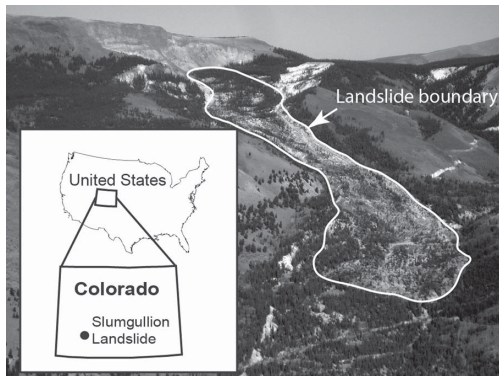


Figure 1. Photograph and location of the Slumgullion landslide.

countries, and is becoming a common practice for landslide research studies (e.g. Tarchi et al. 2003a, b, Antonello et al. 2004, Barla et al. 2010, Gischig et al. 2011).

We used the IBIS-L GB-InSAR system developed by IDS (Ingegneria dei Sistemi, Pisa) to study kinematics of the complex Slumgullion landslide located in the San Juan Mountains of Colorado (Fig. 1). The landslide is sparsely vegetated and has many individual kinematic elements (Fleming et al. 1999) with annual speeds that vary between 0.5–7 m/yr (Coe et al. 2003). Our study was directed toward evaluating GB-InSAR for identifying subtle differences in the kinematics of the landslide during a short time period, and using the results to better understand how interactions of kinematic elements are related to overall landslide motion.

2 THE SLUMGULLION LANDSLIDE

The Slumgullion landslide (Fig. 1) occurs in variably weathered Tertiary basalt, rhyolite, and andesite; rhyolite and andesite units generally are highly modified by acid-sulfate hydrothermal alteration (Lipman 1976, Diehl & Schuster 1996) and weathered to clayey, silty sand. The landslide is 3.9 km long, averages about 300 m wide, and has estimated average thickness of 13 m and volume of $20 \times 10^6 \text{ m}^3$ (Parise & Guzzi 1992). The ground surface along the landslide ranges in elevation between 3000–3700 m and has a mean inclination of about 8° . Being in the montane and subalpine ecological zones (Love 1970), yet with a highly disrupted ground surface due to the slide's persistent movement, the landslide is sporadically covered (~20%) by Englemann spruce and aspen

trees, which were in leaf during our surveys. The areas adjacent to the landslide are nearly entirely covered by mature spruce and aspen. The landslide moves persistently (Fleming et al. 1999, Coe et al. 2003, Schulz et al. 2007) and appears to have done so for at least the past 300 yrs (Varnes & Savage 1996). Pore-water pressures clearly control landslide speed (Varnes & Savage 1996, Coe et al. 2003, Schulz et al. 2007), with significant rainfall or snowmelt causing landslide acceleration within hours and elevated speeds lasting for weeks-months. Shear-zone dilation and consequent pore-water pressure decrease appear to retard acceleration (Schulz et al. 2007) while onset of low atmospheric tides appears to trigger daily acceleration episodes (Schulz et al. 2009).

Slumgullion moves by sliding along bounding faults. Detailed mapping performed by Fleming et al. (1999) shows that many individual kinematic elements comprise the landslide and these are bounded by discrete faults. The locations of faults and the elements they bound appear to stay fixed in space while the landslide continues its movement, causing Fleming et al. (1999) to hypothesize that the landslide's boundary geometry remains fixed in space and results in formation and persistence of the kinematic elements; recent work by Coe et al. (2009) provides evidence that this hypothesis is correct. We used the structural mapping of Fleming et al. (1999) to delineate the landslide's major kinematic elements (Fig. 2). Smith (1993) used aerial photographs from 1985 and 1990 to measure displacement of hundreds of surface features on the landslide, and Table 1 shows average speeds from Smith (1993) for each kinematic element that we mapped using Fleming et al. (1999). As indicated on Table 1 and Figure 2, the central part of the slide moves fastest and the slide head moves more slowly than the toe; average speeds of the kinematic elements were 1.9–14.4 mm/d during 1985–1990.

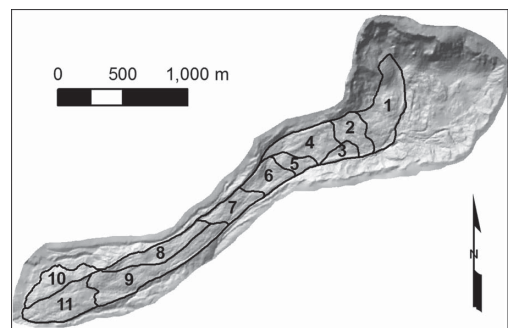


Figure 2. Map showing major kinematic elements comprising the Slumgullion landslide.

Table 1. 1985–1990 average speeds by kinematic element.

| Element | Speed (mm/d) | Standard deviation (mm/d) |
|------------------|--------------|---------------------------|
| Entire landslide | 7.4 | 3.8 |
| 1 | 1.9 | 1.1 |
| 2 | 3.3 | 0.7 |
| 3 | 3.9 | 0.4 |
| 4 | 4.4 | 1.4 |
| 5 | 6.7 | 0.8 |
| 6 | 10.6 | 2.4 |
| 7 | 14.4 | 2.0 |
| 8 | 9.8 | 1.1 |
| 9 | 10.0 | 2.4 |
| 10 | 2.9 | 1.0 |
| 11 | 5.4 | 1.0 |

3 MONITORING INSTRUMENTS

The GB-InSAR equipment used, called IBIS-L and manufactured by IDS, consists of a portable radar unit working in Ku frequency band that slides along a 2-m-long rail while taking measurements. The system is composed of the radar unit, consisting of the linear scanner, radar sensor and power supply module, and a rugged laptop housed inside the power supply module (Fig. 3).

The system utilizes the software IBIS-L Controller, which is used to setup the acquisition parameters and the system diagnostics, and IBIS Guardian for data processing and output visualization. Guardian is devoted to the real-time processing of radar data with automatic atmospheric corrections and it is able to provide fully geo-referenced outputs in the form of displacement and velocity maps. The system can generate alarms based on velocity data and user-defined levels, and also allows multiple alarm criteria for user-defined spatial zones. All the outputs of the software can be exported to common GIS, CAD, or mine planning software. Table 2 shows the main features of the system. It must be noted that GBInSAR measures only the component of displacement along the Line of Sight (LoS) of the radar. Negative displacement values indicate a movement toward the sensor (shortening along the LoS), while positive displacement values indicate a movement away from the sensor (lengthening along the LoS).

The major technical advances of the IBIS-L system are the interferometric processing techniques. The employed algorithms utilize statistical analyses to select a grid of high quality pixels (Persistent Scatterers, PS) for removing atmospheric artifacts from the interferometric

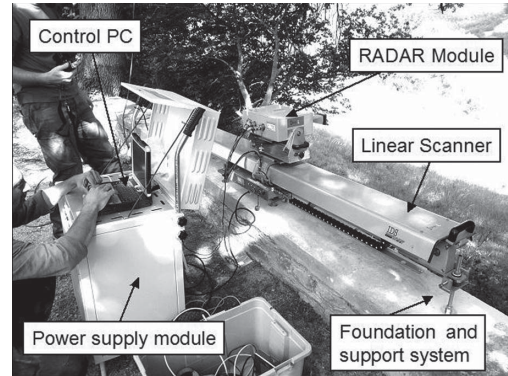


Figure 3. Photograph showing main components of the GB-InSAR system.

Table 2. GB-InSAR characteristics (IDS, IBIS-L model).

| Characteristic | Description |
|-----------------------|---------------------------------------|
| Frequency | Ku band (available also in X band) |
| Radar type | Stepped freq. cont. wave (SF-CW) |
| Operative range | [10–4000] m |
| Range resolution | 0.75 (0.5) m |
| Cross-range res. | 4.38 mrad |
| Displ. accuracy | up to 0.1 mm |
| Acquisition time | ≥5 min |
| Phase ambiguity limit | ~4.4 mm |
| Installation time | ~2 h |
| Power supply | 24 VDC or electrical network |
| Size | 250 × 100 × 100 cm |
| Weight | ~200 Kg |
| Power consumption | 70 W |

signal. Through combined temporal and spatial analyses, the approach exploits differences between the time and space characteristics related to ground displacements and those related to atmospheric artifacts. Additionally, the algorithms allow for an automatic estimation of the atmospheric artifacts for all of the stable and moving points contained in the radar image to achieve a closer and more complex model of these artifacts and remove them from the phase signal. The advanced processing algorithms extend the operating range of the radar to 4 km. This range is ideal for most landslide applications because it allows for complete coverage of a range of landslide sizes and remote installation in stable locations. Conventional approaches used in optical systems such as robotic total stations and

for other radar systems, generally do not work as well over long ranges or with highly variable atmospheric conditions.

At Slumgullion, we located the IBIS-L on the crest of the landslide headscarp with a downslope view of nearly all of the landslide, although downward look angles of 10–24° along the average 8° slope of the landslide surface were not ideal (Fig. 4). We bolted the IBIS-L to ~200 kg of concrete blocks placed on crushed gravel compacted on in-situ weathered basalt. A gasoline-powered generator supplied electricity to the system. Data acquisition was set to the maximum range (4 km) with a pixel resolution of 1 m. Table 3 provides additional acquisition parameters. In total, 690 full scans of the landslide were made during the 4.6-day campaign.

During GB-InSAR surveying, we continuously measured landslide movement at three locations (Fig. 5) using cable extensometers and we surveyed 13 monuments using differential GPS at the onset and completion of GB-InSAR surveying. We also surveyed the IBIS-L position using differential GPS.

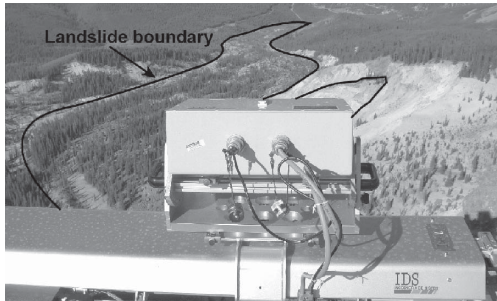


Figure 4. Photograph showing the IBIS-L and its view of the Slumgullion landslide.

Table 3. GB-InSAR data acquisition parameters.

| Parameter | Value |
|------------------------|------------------------------------|
| Maximum distance | 4000 [m] |
| Range resolution | 1 [m] |
| Cross-range resolution | 4.4 [mrad] |
| Sampling time | 9.40 [min · s] |
| Antenna type | Horn 23 [dB] |
| Vertical tilt | 17 [deg] |
| Bearing | 236.57 [deg] |
| Scenario position | [400; 4000] [m] [-18; 24] [deg] |
| Images acquired | 690 |
| Acquisition duration | 4.6 day |

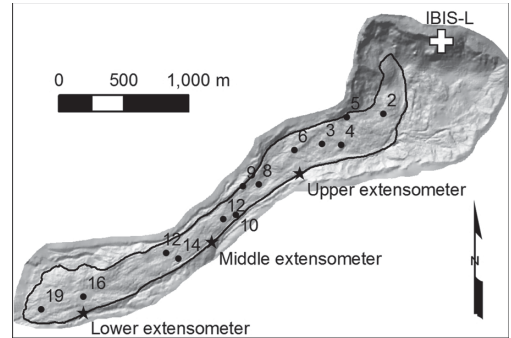


Figure 5. Map showing locations of in-situ instrumentation and survey monuments.

4 RESULTS

The IBIS-L continuously surveyed the landslide during the 5-day campaign without human intervention. Weather during the campaign ranged from calm and clear to very windy with thunderstorms, and temperatures were between 5–19° C. Each scan obtained usable measurements for about 41,000 pixels on the landslide; usable pixels were selected based on the power of the return signal. Figure 7 shows the total LoS displacements measured by the system.

Displacements measured by the IBIS-L compare favorably with those from extensometers but less favorably with those from GPS surveys, although the general displacement trends measured by GPS and GB-InSAR are similar (Fig. 7). The GPS surveys have more error (± 1 cm) than the extensometer measurements (± 1 mm). The apparent uphill movements of GPS monuments 2, 5, and 6 highlight the uncertainty in the GPS results. Additionally, close inspection of the GB-InSAR results (Fig. 8) indicates that some points are inaccurate, with some locations having apparently moved upslope during the the survey campaign. Those points are likely due to signal returns from unstable objects, such as areas covered by vegetation. Downslope movement is expected for all points on the landslide. We show (Fig. 7) mean displacements for the three GB-InSAR measurements nearest each extensometer or GPS monument to partly account for possible erroneous point measurements in the GB-InSAR data.

The IBIS-L results suggest a great deal of differential displacement across the landslide, with total displacements ranging from ~0–15 cm, assuming negative movements are erroneous. The abrupt changes in displacement measured by the IBIS-L apparent in Figure 6 compare very well with the boundaries of kinematic elements delineated from

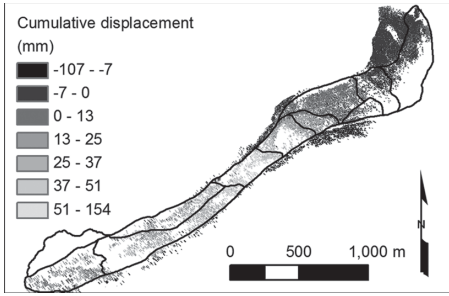


Figure 6. Map showing total displacements measured by the IBIS-L during the survey campaign.

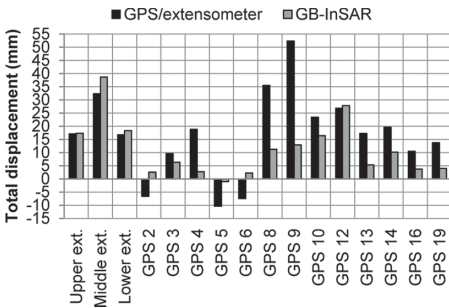


Figure 7. Chart comparing displacement measurements made by the IBIS-L, GPS surveys, and extensometers. GPS and extensometer displacements are relative to the IBIS-L LoS.

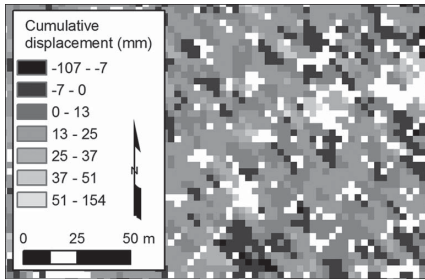


Figure 8. Large-scale map showing variability of displacement measurements acquired by the IBIS-L.

the Fleming et al. (1999) detailed structure map of the landslide. The relative speeds for each element determined from GB-InSAR were slower than those measured by Smith (1993) for the period 1985–1990, but the trends in speeds by kinematic element are similar (Fig. 9). However, normalizing the speeds obtained from the GB-InSAR surveys by those from Smith (1993) indicates that the differences in speed between the two datasets are great near the landslide head and small near the landslide toe (Fig. 10).

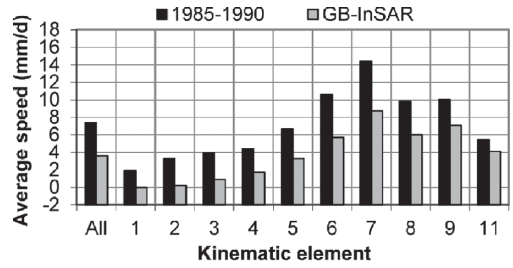


Figure 9. Average speeds of kinematic elements (Fig. 2) measured by the IBIS-L and from aerial photographs (Smith 1993). No InSAR data were acquired for element 10.

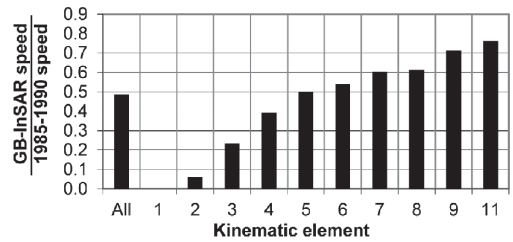


Figure 10. Ratios of the average speeds of kinematic elements (Fig. 2) measured by the IBIS-L to those measured from aerial photographs (Smith 1993). No InSAR data were acquired for element 10.

5 DISCUSSION

The quality of results obtained from the GB-InSAR surveys varied with temporal and spatial scale. For example, the surveys clearly identified the moving landslide and kinematic elements of which the slide is composed, and daily displacements compared well with measurements from extensometers. These favorable results were apparent on the first day of surveying. For example, Figure 11 shows total displacements measured after about 16 hrs, and the kinematic elements were already clear. Thus, GB-InSAR was able to provide kinematic data in one day that were in many ways comparable to data obtained during several months of field mappings. At the other end of the spectrum, many individual GB-InSAR measurements characterized by lower coherence provided more ambiguous results (e.g., Fig. 8), with individual points supposedly moving uphill during the duration of the campaign while others moved uphill for short time periods. The opportunistic nature of GB-InSAR (no need for artificial reflectors) implies the need to properly select the high quality pixels masking out the areas where the quality of the signal is not sufficient to

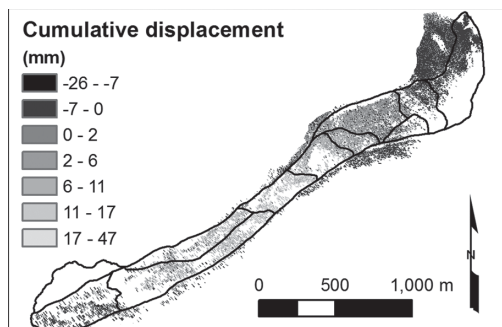


Figure 11. Map showing total displacements measured by the IBIS-L during the first 16 hrs of surveying.

provide accurate measurements. Future efforts will be directed toward identification and extraction of only high quality data by using on a selection mask calculated on the temporal coherence of the data all over the entire dataset.

The GB-InSAR data permit some interesting observations to be made, which we are only beginning to analyze. For example, the landslide moved ~9–130 m during the ~18 yrs since the Fleming et al. (1996) field mapping was completed in 1993, yet the kinematic elements identified during our survey appear to remain the same. This similarity provides additional evidence that landslide boundary geometry largely controls the existence and nature of internal structures and that the boundary geometry remains unchanged (Fleming et al. 1996, Coe et al. 2009). However, the speeds measured during our survey were much lower than those measured by Smith (1993) between 1985–1990; on average, the landslide during our survey moved at 49% of the average speed measured between 1985–1990 (Fig. 10). GPS surveys performed annually by Coe (in press) also show significant slowing between 1998 and 2011; hence, there is no reason to doubt the GB-InSAR cumulative displacement measurements. In addition, our measurements indicate that the landslide head was moving much more slowly during 2011 than during 1985–1990, whereas the landslide toe was moving nearly as quickly (Fig. 10). We believe that these differences are real, rather than artifacts, because there is no similar trend evident between GB-InSAR results and those from GPS monuments and extensometers, which are distributed along the length of the landslide. The marked slowing of the landslide head relative to the middle part and toe may be early manifestations of conclusions made by Coe (in press). His analyses of landslide movement during 1998–2011, historical and projected future air temperature and precipitation suggest that the landslide will stop moving a few centuries from now (based on projected increasing

temperatures), but cessation of movement will begin at the landslide head ~2060 AD and propagate downslope. Perhaps the behavior he predicts for the landslide is occurring already. Our continued analyses of the GB-InSAR data should provide additional information regarding the landslide's kinematics and conditions affecting its movement.

6 CONCLUSION

Knowledge of landslide kinematics is critical for understanding landsliding mechanisms and developing mitigation strategies. We used the IBIS-L GB-InSAR system for a 5-day period during June 2010 to measure movement of the 3.9-km long Slumgullion landslide located in Colorado, USA. Previous studies (Fleming et al. 1996, Smith 1993) provided data with which we delineated kinematic elements comprising the landslide and their average speeds during 1985–1990. Measurements of three extensometers and GPS surveys of 13 monuments distributed across the landslide surface provided a means to check the results from the GB-InSAR surveys. The IBIS-L ran autonomously and continuously during the campaign, acquiring full scans of the landslide every 9 min 40 s. Before the first day of surveying was completed, kinematic elements could be identified that correlated spatially with those identified from results of previous studies. The elements identified during our survey campaign were spatially consistent with those mapped ~18 yrs previous, suggesting that landslide boundary geometry remains fixed in time and space and largely determines internal kinematics. Displacements measured by the GB-InSAR system on areas not covered by vegetation correlated well with those measured using extensometers and GPS. Average landslide speeds were significantly lower during our campaign compared to 1985–1990, and the differences were greatest toward the landslide head. These results are similar to those obtained from GPS surveys between 1998–2011 (Coe in press) and suggest that slowing and eventual stoppage of the landslide predicted by Coe (in press) may be occurring already.

DISCLAIMER

The use of trade, product, industry, or firm names herein is for descriptive purposes only and does not imply endorsement by the US Government.

REFERENCES

- Antonello, G., Casagli, N., Farina, P., Leva, D., Nico, G., Sieber, A.J. & Tarchi, D. 2004. Ground-based SAR interferometry for monitoring mass movements. *Landslides* 1: 21–28.

- Barla G., Antolini F., Barla M., Mensi E., Piovano G. 2010. Monitoring of the Beauregard landslide (Aosta Valley, Italy) using advanced and conventional techniques. *Engineering Geology* 116: (3–4) 218–235.
- Coe, J.A. in press. Regional moisture balance control of landslide motion: Implications for landslide forecasting in a changing climate. *Geology*.
- Coe, J.A., Ellis, W.L., Godt, J.W., Savage, W.Z., Savage, J.E., Michael, J.A., Kibler, J.D., Powers, P.S., Lidke, D.J. & Debray, S. 2003. Seasonal movement of the Slumgullion landslide determined from Global Positioning System surveys and field instrumentation, July 1998–March 2002. *Engineering Geology* 68: 67–101.
- Coe, J.A., McKenna, J.P., Godt, J.W. & Baum, R.L. 2009. Basal-topographic control of stationary ponds on a continuously moving landslide. *Earth Surface Processes and Landforms* 34: 264–279.
- Diehl, S.F. & Schuster, R.L. 1996. Preliminary geologic map and alteration mineralogy of the main scarp of the Slumgullion landslide. In: D.J. Varnes & W.Z. Savage (eds), *The Slumgullion earth flow: A large-scale natural laboratory*. U.S. Geological Survey Bulletin 2130: 13–19.
- Fleming, R.W., Baum, R.L. & Giardino, M. 1999. Map and description of the active part of the Slumgullion landslide, Hinsdale County, Colorado. *US Geological Survey Geologic Investigations Series Map I-2672*.
- Gischig, V., Amann, F., Moore, J.R., Loew, S., Eisenbeiss, H. & Stempfhuber, W. 2011. Composite rock slope kinematics at the current Randa instability, Switzerland, based on remote sensing and numerical modeling. *Engineering Geology* 118: 37–53.
- Lipman, P.W. 1976. Geologic map of the Lake City caldera area, western San Juan Mountains, southwestern Colorado. *U.S. Geological Survey Miscellaneous Investigation Series Map I-962*.
- Love, D. 1970. Subarctic and subalpine: where and what? *Arctic and Alpine Research* 2: 63–73.
- Parise, M. & Guzzi, R. 1992. Volume and shape of the active and inactive parts of the Slumgullion landslide, Hinsdale County, Colorado. *U.S. Geological Survey Open-File Report 92-216*.
- Schulz, W.H., McKenna, J.P., Biavati, G. & Kibler, J.D. 2007. Relations between hydrology and velocity of a continuously moving landslide—evidence of pore-pressure feedback regulating landslide motion? *Landslides* 6(3): 181–190.
- Schulz, W.H., Kean, J.W. & Wang, G. 2009. Landslide movement in southwest Colorado triggered by atmospheric tides: *Nature Geoscience* 2(12): 863–866.
- Smith, W.K. 1993. Photogrammetric determination of movement on the Slumgullion slide, Hinsdale County, Colorado, 1985–1990. *U.S. Geological Survey Open-File Report 93-597*.
- Spiker, E.C. & Gori, P.L. 2003. National landslide hazards mitigation strategy—a framework for loss reduction. *U.S. Geological Survey Circular 1244*.
- Tarchi, D., Casagli, N., Fanti, R., Leva, D.D., Luzi, G., Pasuto, A., Pieraccini, M. & Silvano, S. 2003a. Landslide monitoring by using ground-based SAR interferometry: an example of application to the Tessina landslide in Italy. *Engineering Geology* 68: 15–30.
- Tarchi, D., Casagli, N., Moretti, S., Leva, D. & Sieber, A.J. 2003b. Monitoring landslide displacements by using ground-based synthetic aperture radar interferometry: application to the Ruinon landslide in the Italian Alps. *Journal of Geophysical Research* 108(B8): ETG 10-1–10-14.
- Varnes, D.J. & Savage, W.Z. 1996. The Slumgullion earth flow: A large-scale natural laboratory. *U.S. Geological Survey Bulletin* 2130.